Understanding surface and subsurface temperature changes induced by tropical cyclones in the Kuroshio

Xin Liu[1] · Jun Wei[1]

Abstract Surface and subsurface temperature changes in the Kuroshio induced by tropical cyclones (TCs) were investigated using both 10-year observational datasets (SST maps and Argo data) and temperature budget analysis of idealized numerical simulations. Although Argo data are very limited during a TC's passage, they provided unique in situ measurements at the subsurface of the Kuroshio. Compared to the surface water in the Kuroshio and in the general ocean, the subsurface water of the Kuroshio shows a rapid temperature warming (recovery) after a TC's passage. Budget analysis on the model simulations suggested that the temperature changes at surface Kuroshio are dominated by the wind-induced vertical mixing, while the subsurface temperature changes are primarily dominated by TC-induced Ekman pumping (downwelling-upwelling-downwelling pattern). The Kuroshio subsurface water is warmed up mainly by the downwelling process, and then transported downstream by strong Kuroshio currents. Sensitivity experiments suggested that the recovery time of the subsurface temperature cooling is more sensitive to TC translation speeds and less sensitive to the Kuroshio current velocities.

✉ Jun Wei
  junwei@pku.edu.cn

[1] Laboratory for Climate and Ocean-Atmosphere Studies, Department of Atmospheric and Oceanic Science, Peking University, Beijing, China

1 Introduction

The Kuroshio current is one of the most important boundary currents in the Pacific Ocean and plays a pivotal role in the regional and global climate system, as it transports a large amount of heat content poleward in the upper ocean (Guo et al. 2003; Hsueh 2000; Nagano et al. 2007; Small et al. 2008). While the large synoptic variability of the Kuroshio received much attention from previous studies (Andres et al. 2008; Miyazawa et al. 2004; Tseng et al. 2012), few studies have been zoomed into its mesoscale changes in weather time scales, especially during a TC's passage. For most of landed TCs in the northwestern Pacific, the Kuroshio is an energetic, warm, and elongated passway that they have to cross over before their landing. Due to sustained cyclonic-rotating winds, a translating TC usually produces vigorous temperature responses in the upper ocean, including within the Kuroshio region (Price 1981; Sriver and Huber 2007; Liu et al. 2008; Zheng et al. 2008; Sanford et al. 2011). In contrast to the open ocean, the pre-existing strong current of the boundary currents, such as the Kuroshio and the Gulf Stream, makes their responses much more complicated (Oey et al. 2006; Wu et al. 2008; Uhlhorn and Shay 2013; Wei et al. 2014).

TCs change ocean temperature mainly through two major processes in the ocean: vertical mixing and upwelling. Vertical mixing is an associated entrainment process in the upper ocean, produced by wind-induced current velocity shear (Shay et al. 2000; Jaimes and Shay 2009). Upwelling can be induced at the ocean surface by TC-induced near-inertial

current oscillations and throughout the water column by Ekman pumping effect induced by TC's cyclonic wind field (Price et al. 1994; Huang et al. 2009). Based on a mixed layer ocean model, Price (1981) found that wind-induced vertical mixing usually dominates the total sea surface temperature (SST) cooling (up to ~85 %) and upwelling accounts for less than 15 %. This model result is supported by observations reported in Jacob et al. (2000). Jullien et al. (2012) found that the vertical mixing largely explains the surface temperature cooling in the open ocean, while the upwelling plays an important role at the subsurface. The upper ocean temperature changes also can be significantly influenced by heat fluxes under TC conditions (Jacob et al. 2000; Sriver and Huber 2007; Huang et al. 2009; Vincent et al. 2012). Overall, the TC-induced temperature cooling often demonstrated a rightward pattern in the satellite images, which was attributed to wind stress vector turned clockwise in time on the right side of the track roughly resonant with the ocean near-inertial oscillations (Price 1981; Shay et al. 1992; Cione and Uhlhorn 2003).

While TC-induced temperature cooling in the open ocean has been well documented in the previous studies, our knowledge of ocean responses in the regions with pre-existing energetic and warm boundary currents (the Kuroshio and the Gulf Stream) is very limited. This can be inferred from inconsistent findings from some relevant studies. Wu et al. (2008) found that no significant temperature cooling in satellite SST maps occurred in the Kuroshio region during typhoon Nari's passage and they attributed it to a deep thermocline of the Kuroshio that prevents the entrainment process. Oey et al. (2006) even reported an abnormal warming in the Loop Current of the Gulf Stream after hurricane Wilma's passage. They attributed it to strong heat and volume transport of the Loop Current enhanced by Wilma. Based on temperature budget analyses on an idealized model, Uhlhorn and Shay (2013) claimed that most of wind energy transferred to ocean mixed layer in the Loop Current is quickly removed by the current, and therefore no significant ocean cooling will occur. However, in contrast to increased volume transport reported by Oey et al. (2006), Uhlhorn and Shay (2012) showed a velocity decrease of 0.18 m/s over a 10-day period of hurricane Lili's passage. Morimoto et al. (2009) found significant temperature cooling (~13 °C) on the shelf beside the Kuroshio and attributed it to intrusions of the Kuroshio subsurface cold water. Sakaida et al. (1998) found 9 °C temperature cooling in the Kuroshio extension area and attributed it to sharp temperature gradient below the surface. In our previous study, we extensively investigated the Kuroshio responses to typhoon Megi (2004), based on a comprehensive temperature budget analysis (Wei et al. 2014). We found that TC-induced SST cooling in the Kuroshio region can be stronger than

that in the open ocean. The underlying mechanism is associated with a large amount of momentum energy released from baroclinic pressure work of the Kuroshio that significantly enhances local vertical mixing.

With the aid of high-resolution satellite-derived SST images, many previous studies well interpreted TC-induced temperature changes, primarily on the ocean surface. Argo program automatically collected nearly in situ temperature profiles in the upper 2000-m global ocean with an interval of a few days and provided a unique opportunity to study ocean subsurface responses to translating TCs (Park et al. 2011; Sun et al. 2012; Vissa et al. 2012; Wu and Chen 2012). Unlike these studies which were all focused on the open ocean, the present study will be focused on understanding the subsurface temperature changes of the Kuroshio by means of 10-year satellite SST images and Argo data during the periods of TCs' passage. Model simulations and temperature budget analysis also were carried out to help better understand the mechanisms underlying the observed subsurface temperature responses in the Kuroshio.

2 Data and model

2.1 Data

The data used in this paper include TC trajectories and intensities, satellite-derived SST maps, and Argo temperature profiles. TC information was obtained from the Joint Typhoon Warning Center (JTWC, http://www.usno.navy.mil/JTWC/), including the best track, locations of TC center, maximum sustained wind speeds, and minimum central pressure. SST maps were obtained from Tropical Rainfall Measuring Mission/Microwave Imager (TRMM/TMI, http://pmm.nasa.gov/TRMM), which provides cloud-penetrating daily SST with a resolution of $0.25° × 0.25°$. Subsurface temperature profiles were obtained from the Argo datasets, provided by the China Argo Real-time Data Center (http://www.argo.org.cn/). Argo datasets provide individual vertical temperature profiles with 1-, 2-, 4-, 5-, or 10-day intervals. According to the periods of each TC, we were able to identify the Argo floats before, during, and after a TC's passage.

2.2 Model configuration

To better interpret the mechanisms of the surface and subsurface temperature changes in the Kuroshio, an ocean model with idealized TCs and Kuroshio was built using the Regional Oceanic Modeling System (ROMS) (Shchepetkin and McWilliams 2005). The model domain spanned 3030 km in the x direction and 6030 km in the y

direction, with a uniform resolution of 15×15 km. The periodic boundary condition was used in the x direction to maintain a persistent Kuroshio current, and Flather open boundary condition (Flather 1976) was applied in the y direction. The initial temperature field was obtained from long-term average temperature on August through P-N (Pollution Nagasaki) section as shown in Fig. 1a. The P-N section is located in the central East China Sea (ECS) monitoring the transport and variability of the Kuroshio, provided by the Nagasaki Marine Observatory of Japan Meteorological Agency (JMA) (Ichikawa and Beardsley 2002; Tseng et al. 2012). Salinity was set to constant (35 psu) throughout the entire model integration. Initial velocity fields were calculated based on the equation of geostrophic balance (Fig. 1b).

The ocean model was forced by an idealized translating TC wind field with a translation speed of $Vs = 5.5$ m/s along the $+y$ direction (Fig. 1e). The wind forcing is an axisymmetric TC whose radial and maximum wind speeds were approximated from 10-year average of JTWC data (Fig. 1c, d). The maximum radial wind speed that is 45 m/s occurred at about 50 km away from the TC center. The model was integrated for a total of 20 days. To focus on the ocean internal processes, heat flux forcing was not included.

3 Results

3.1 Observed ocean temperature response to TCs

Surface and subsurface temperature responses were first analyzed from SST maps and Argo profiles, respectively, for those TCs moving perpendicularly across the Kuroshio. A total 22 such TCs were identified from 2001 to 2010, with tracks nearly perpendicular to the Kuroshio in the ECS (Fig. 2a). In order to determine TC-induced temperature changes in the Kuroshio region and in a general ocean region, we marked two regions accordingly in Fig. 2a. Red box outlines the Kuroshio region, and the blue one denotes the general ocean. As the two regions are very close (~50 km), TC intensity changes were neglected when they passed over the two regions.

Surface temperature changes SST cooling and recovery time for the selected TCs during 2001–2010 are summarized in Table 1. The SST cooling was calculated within 150 km on the right-hand side of TC tracks. Statistical results suggested that the SST cooling in the Kuroshio region (marked as "IN_KS") ranges from 0.61 to 4.93 °C, with a mean of 2.09 °C. On the other hand, the SST cooling in the general
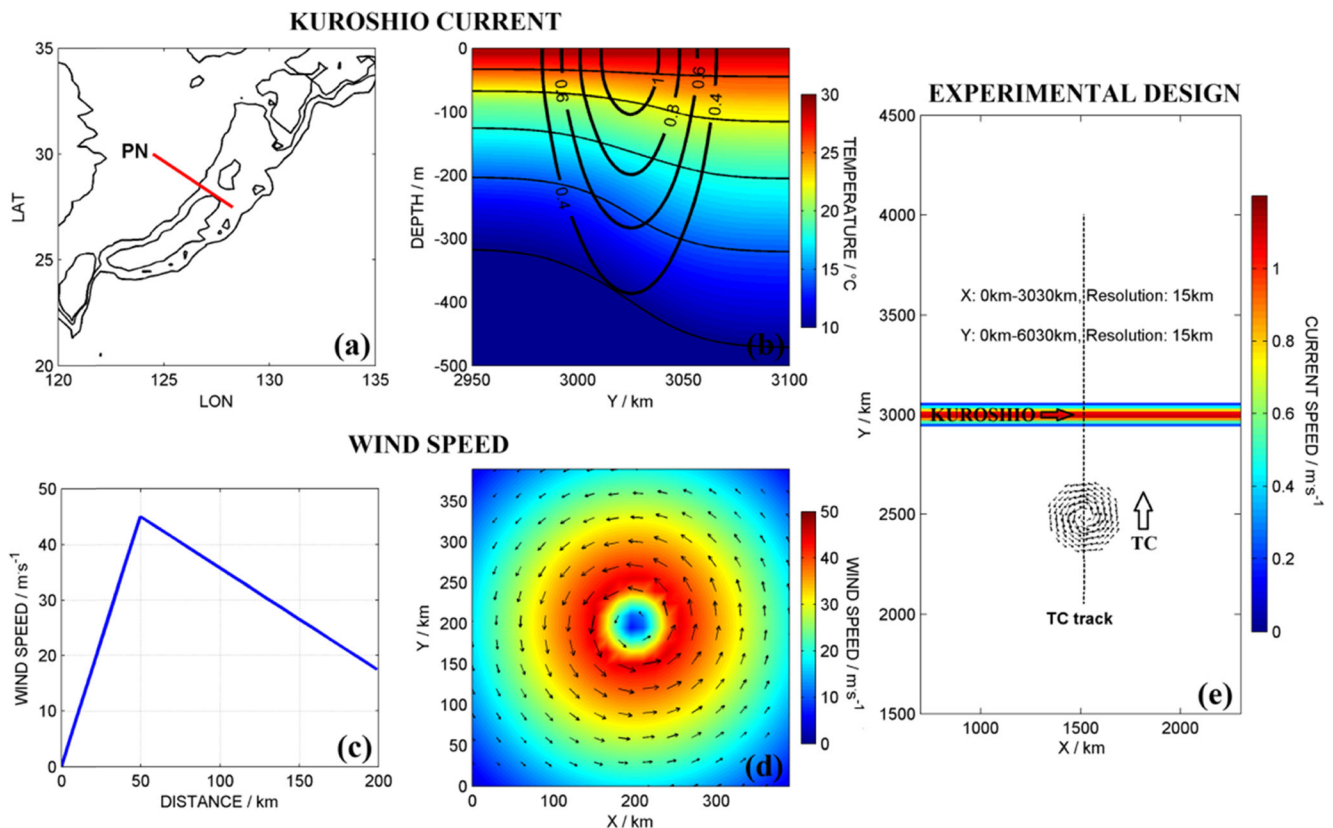

Fig. 1 **a** Location of P-N section. **b** Model initial temperature (*color shading* and *contours without numbers*) and geostrophic currents (*contours with numbers*). **c** Idealized radial wind speed. **d** Idealized TC bottom wind field. **e** Model domain and schematics of simulations for TC-Kuroshio interaction. *Color shading* indicates the current speed of the Kuroshio
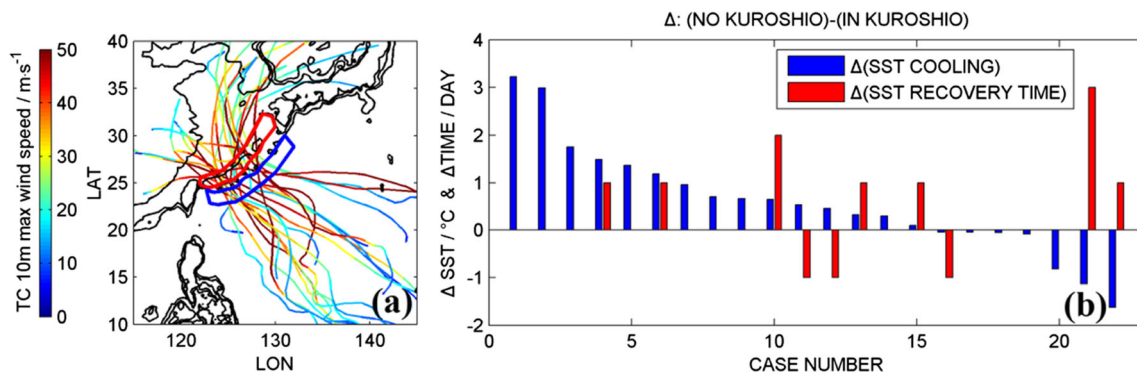
Fig. 2 **a** Trajectories of 22 selected TCs colored by their intensities. *Red box* outlines the Kuroshio region, and *blue box* outlines the general ocean outside the Kuroshio. **b** Difference of SST cooling (*blue bars*) and recovery time (*red bars*) between in the general ocean and in the Kuroshio

ocean region (marked as "NO_KS") is apparently stronger than that in the Kuroshio region, with average difference of 0.58 °C. Differences of the SST cooling and recovery time for individual TC between the two regions are shown in Fig. 2b. For most of the selected TCs (15 out of 22 TCs), SST cooling is stronger in the general ocean than that in the Kuroshio. On the other hand, SST cooling in the Kuroshio generally recovers faster than that in the general ocean.

Subsurface temperature changes According to the passages of the 22 selected TCs, 7 Argo floats were found located in the Kuroshio region marked in the blue box in Fig. 2a. Seven additional Argo floats in the open ocean during the same periods were also selected for comparison. Figure 3 shows locations and temperature profiles of the 14 Argo floats before, during, and after the TCs' passage. Although associated with different TCs, the Argo profiles demonstrate the nearly in situ temperature changes during passages of TCs over the Kuroshio and the general ocean. It is shown that the mixed layer depth is generally deeper in the Kuroshio than that in the general ocean before the TC passage (green lines in each plot). During TC passage, wind-induced vertical entrainment cools the temperature in the upper ocean and pushes the mixed layer depths downward (blue lines). After TC passage, the temperature profiles (red lines) recover with different degrees at different stations, but with apparent temperature warming at the

Table 1 Satellite-derived SST cooling (°C) and recovery time (day)

	Min. cooling	Max. cooling	Ave. cooling	STD
ΔSST (NO_KS)	0.52	5.84	2.68	1.40
ΔSST (IN_KS)	0.61	4.93	2.09	0.93
ΔSST (NO_KS - IN_KS)	−1.63	3.22	0.58	1.15
RT (NO_KS)	1.00	8.00	4.36	2.11
RT (IN_KS)	1.00	7.00	4.05	1.94
ΔRT (NO_KS - IN_KS)	−1.00	3.00	0.32	0.95

NO_KS General Ocean, *IN_KS* Kuroshio, *RT* recovery time

subsurface water of the Kuroshio (Fig. 3c). To better distinguish subsurface temperature warming, the temperature profiles were shaded with yellow color within the mixed layer and pink color below. The mixed layer depth here is defined as the depth whose temperature is 0.5 °C less than the sea surface temperature based on blue lines. Note that in this paper, we particularly defined the subsurface as depths below the mixed layer depth until 200-m depth. Table 2 summaries the surface and subsurface temperature changes shown in Fig. 3. It can be seen that the average temperature warming (recovery) at the surface of the Kuroshio (1.24 °C) is slightly less than that in the general ocean (1.39 °C), which is generally consistent with the results derived from the statistical SST maps (Table 1). In contrast, the average temperature warming at the subsurface of the Kuroshio (3.52 °C) is much larger than that in the general ocean (1.52 °C). To the best of our knowledge, this finding had not been reported by any previous studies.

3.2 Model simulations

Although Argo data are very limited during time periods of the selected TCs, the subsurface temperature warming is prominent in the Kuroshio region compared to the ambient water. To better understand the mechanism underlying the phenomenon, an idealized model experiment with an idealized Kuroshio current forced by a translating TC was carried out (see Sect. 2.2 for detailed model configurations). Figure 4 shows a snapshot of ocean surface and vertical sections of the simulated temperature and velocity at day 5.5. The surface velocity demonstrates a convergence-divergence-convergence pattern (near-inertial oscillations) driven by the translating TC wind forcing. SST cooling occurred mainly along the right-hand side of the TC track, primarily due to resonant coupling between the clockwise-rotating wind stress and near-inertial current oscillations (Price 1981). In the Kuroshio region, the SST cooling was transported downstream by the current. In the vertical sections, TC winds mixed and cooled the upper ocean and deepened the thermocline from 20 to 100 m.
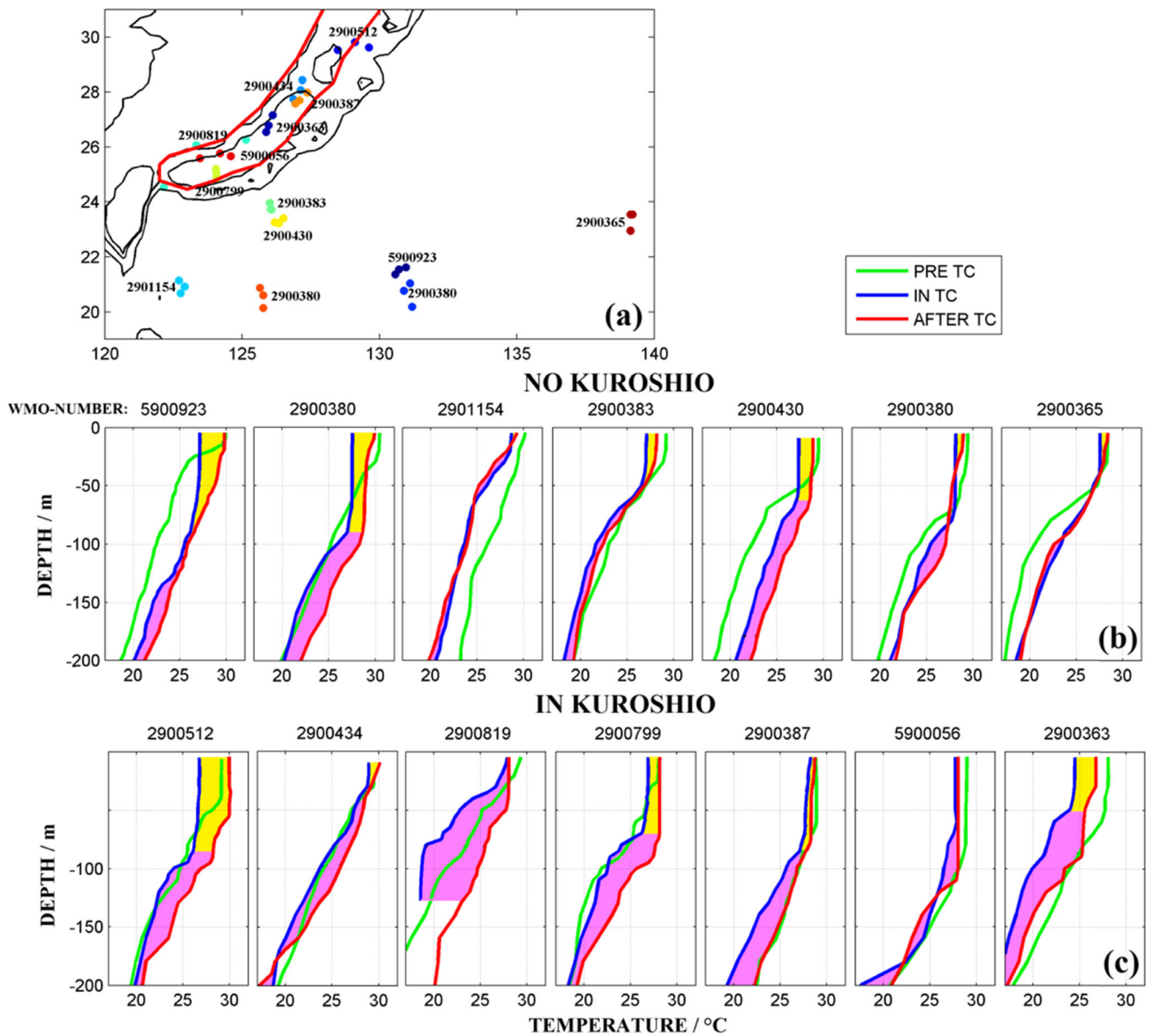
🔻 Springer

Fig. 3 **a** Locations of Argo floats marked by WMO numbers. **b** Argo temperature profiles during time periods of pre-TC (*green lines*), in-TC (*blue lines*), or after-TC (*red lines*) in the general ocean and **c** in the Kuroshio. Surface and subsurface temperature changes are marked, respectively, by *yellow* and *pink shadings*. The surface and subsurface are separated by the mixed layer depth which is defined as a depth with temperature 0.5° less than that in the surface

Figure 5 compares vertical temperature profiles before, during, and after the TC passage. In the general ocean, the temperature response is essentially similar to the Argo profiles (Fig. 3b). The TC-induced temperature cooling occurred in the upper 40 m mainly due to the entrainment process. It can be seen that the entrainment process is

Table 2 Surface and subsurface temperature recovery time derived from Argo profiles

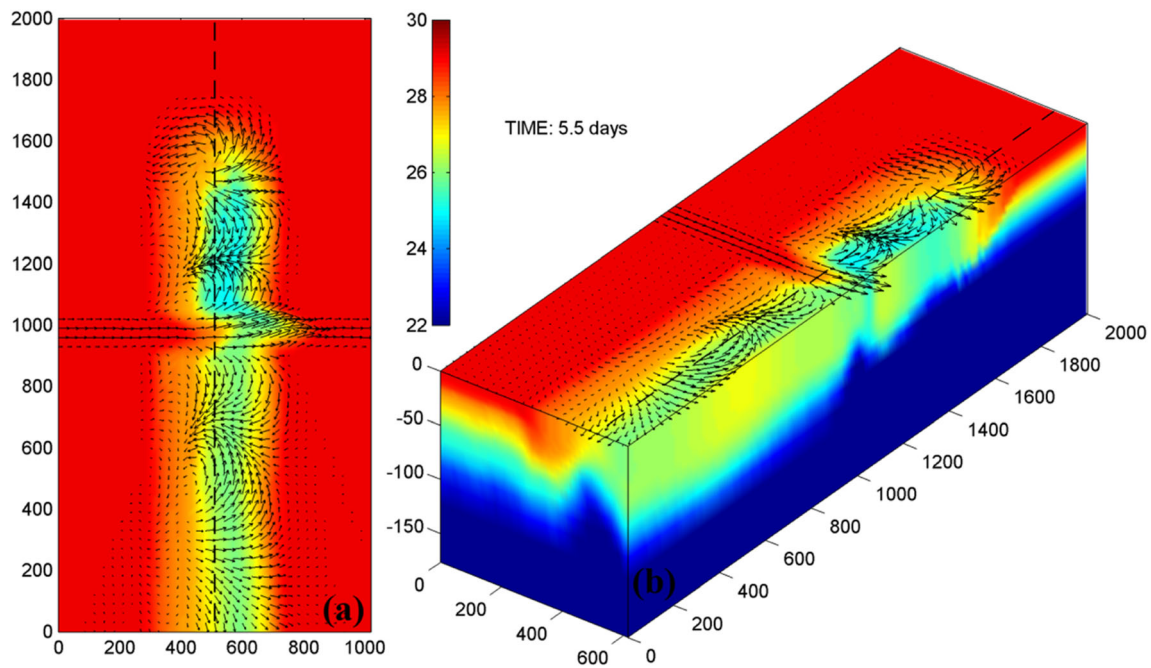| General ocean	5900923	2900380	2901154	2900383	2900430	2900380	2900365	Average
Surface (°C)	2.57	2.33	0.60	1.11	1.52	0.76	0.82	1.39
Subsurface (°C)	1.54	3.08	0.89	0.99	1.78	1.75	0.73	1.54
Kuroshio	2900512	2900434	2900819	2900799	2900387	5900056	2900363	Average
Surface (°C)	3.20	1.21	0.01	1.26	0.47	0.30	2.27	1.24
Subsurface (°C)	3.31	2.13	6.37	4.68	2.48	1.57	4.07	3.52

Fig. 4 Model simulated temperature and velocity of TC-Kuroshio interaction at **a** sea surface and **b** vertical sections

irreversible without any other external forcing, referred from the nearly overlapped blue and red lines. In contrast, in the Kuroshio, the temperature cooling is throughout the water column (blue line) and warms up (recovery) dramatically. Again, similar to the Argo profiles shown in Fig. 3c, the simulated subsurface temperature warming is also much more prominent than that within the surface-mixed layer. Figure 5c indicates that the subsurface temperature warming (recovery) time scale is about 1.2 day.

Figure 6 zooms in the vertical temperature sections (x-z) along the axis of the Kuroshio current during the TC passage. The temperature profile at day 0 indicates the initial state with a mixed layer of 20 m deep. At day 0.125 when the TC approached the Kuroshio, the mixed layer was deepened by the wind-induced vertical mixing, which indicates a typical entrainment process. At day 0.75, the entrainment process continued to mix surface warm water downward on the both side of the TC center. At the same time, remarkable temperature cooling occurred around the TC center. The cold water
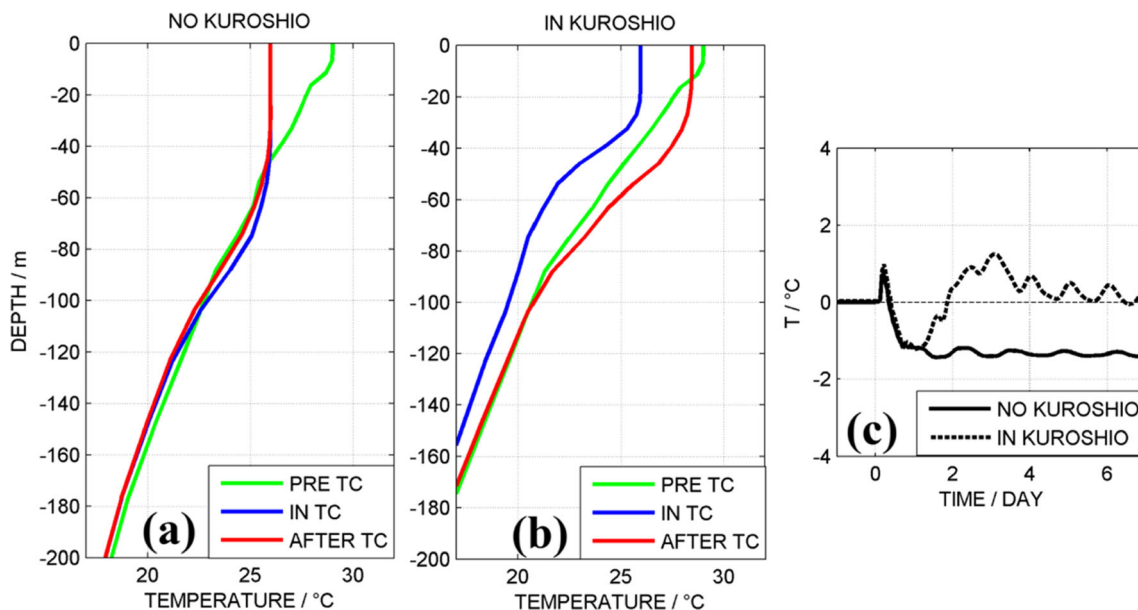

Fig. 5 Model simulated temperature profiles before, during, and after TC passage **a** in the general ocean outside the Kuroshio and **b** inside the Kuroshio. **c** Temperature changes at 26.7-m depth in the general ocean and in the Kuroshio
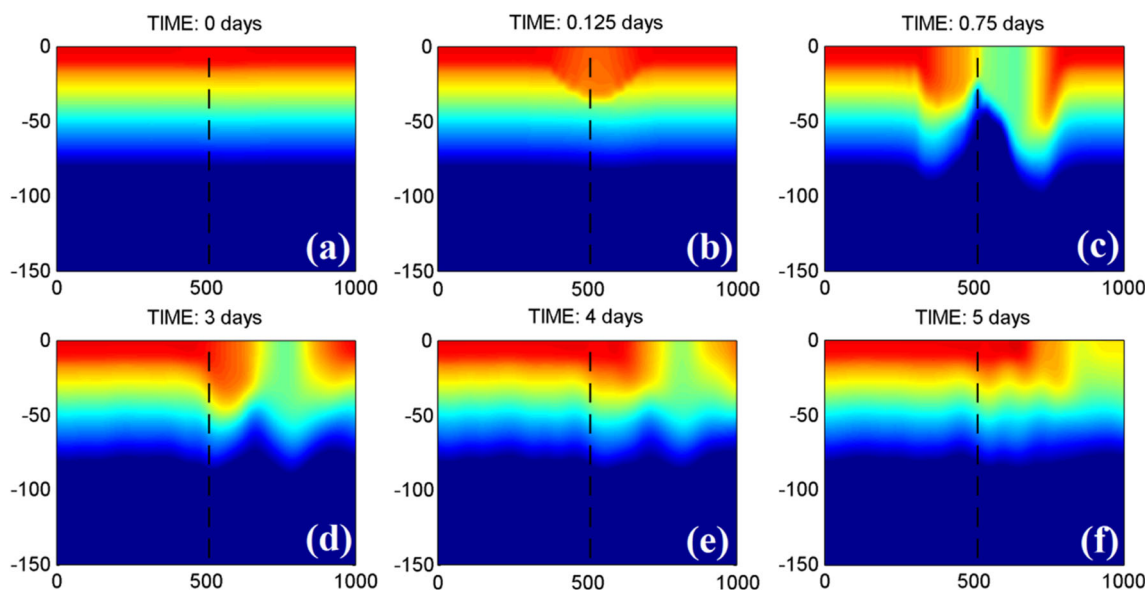
Fig. 6 Vertical sections (x-z) of temperature along the axis of the Kuroshio current during TC passage at **a** day 0, **b** day 0.125, **c** day 0.75, **d** day 3, **e** day 4, and **f** day 5. *Dash lines* indicate the location of TC center

was apparently from the deep ocean indicated by a shoaling thermocline. During days 3–5, such a temperature pattern was transported to the east (downstream) by the Kuroshio, diffused gradually with ambient water.

3.3 Budget analysis for temperature cooling

To further interpret the simulated temperature pattern, a temperature budget analysis was carried out based on the primitive temperature equation following (Wei et al. 2014).

$$\underbrace{\frac{\partial T}{\partial t}}_{T} = -\underbrace{\left(u\frac{\partial T}{\partial x} + v\frac{\partial T}{\partial y} + w\frac{\partial T}{\partial z}\right)}_{ADV} + \underbrace{\frac{\partial}{\partial x}\left(A_h\frac{\partial T}{\partial x}\right) + \frac{\partial}{\partial y}\left(A_h\frac{\partial T}{\partial y}\right)}_{HDIF}$$
$$+ \underbrace{\frac{\partial}{\partial z}\left(K_h\frac{\partial T}{\partial z}\right)}_{VDIF} \tag{1}$$

The left-hand term is the rate of temperature changes. The right-hand side terms are advection (ADV), horizontal diffusion (HDIF), and vertical diffusion/mixing (VDIF), respectively. Note that the formula ignores the heat flux forcing since it is not included in the model. TC-induced temperature changes are primarily contributed by the vertical mixing term (entrainment) and the advection term (upwelling/downwelling), while the horizontal diffusion term is usually negligible (Price 1981; Jacob et al. 2000; Uhlhorn and Shay 2013; Wei et al. 2014).

Figure 7 shows the vertical sections for each individual term except HDIF term. Note that for a better comparison, initial values were subtracted from each term. At day 0.125 (before TC passage), the temperature changes were determined by the vertical mixing (T-DIFF). The entrainment process cooled the surface water and warmed up the subsurface water. At day 0.75 (during TC passage), the vertical mixing term dominated the surface temperature changes, and the advection term (upwelling/downwelling) dominated the water column at the subsurface. It is shown that the advection-induced subsurface temperature cooling is maximized at about 50 m deep near the TC center, compensated by temperature warming on the both sides. This implies a cyclonic circulation on the right-hand side of the TC center and an anticyclonic circulation on the left-hand side. The surface cooling in the T-ADV term is caused by surface current divergences associated with near-inertial motions (Fig. 4a). The vertical mixing term contributes primarily to the surface cooling, maximized toward the right-hand side of the TC center. At day 3 (after TC passage), the temperature changes in the general ocean basically maintained the same pattern as day 0.75, while the temperature changes in the Kuroshio showed a much different pattern for the advection term. Due to strong eastward currents of the Kuroshio, the upstream downwelling-induced warm water was carried over to the east and warmed up the entire upper 50 m around TC center.

A schematic is shown in Fig. 8 to qualitatively demonstrate the processes in the Kuroshio. As a TC is approaching the Kuroshio, the temperature changes in the Kuroshio are mainly determined by the entrainment process induced by weak TC peripheral winds. During the TC passage, strong winds trigger the vertical mixing at the ocean surface and the Ekman pumping (upwelling/downwelling) at the subsurface. After
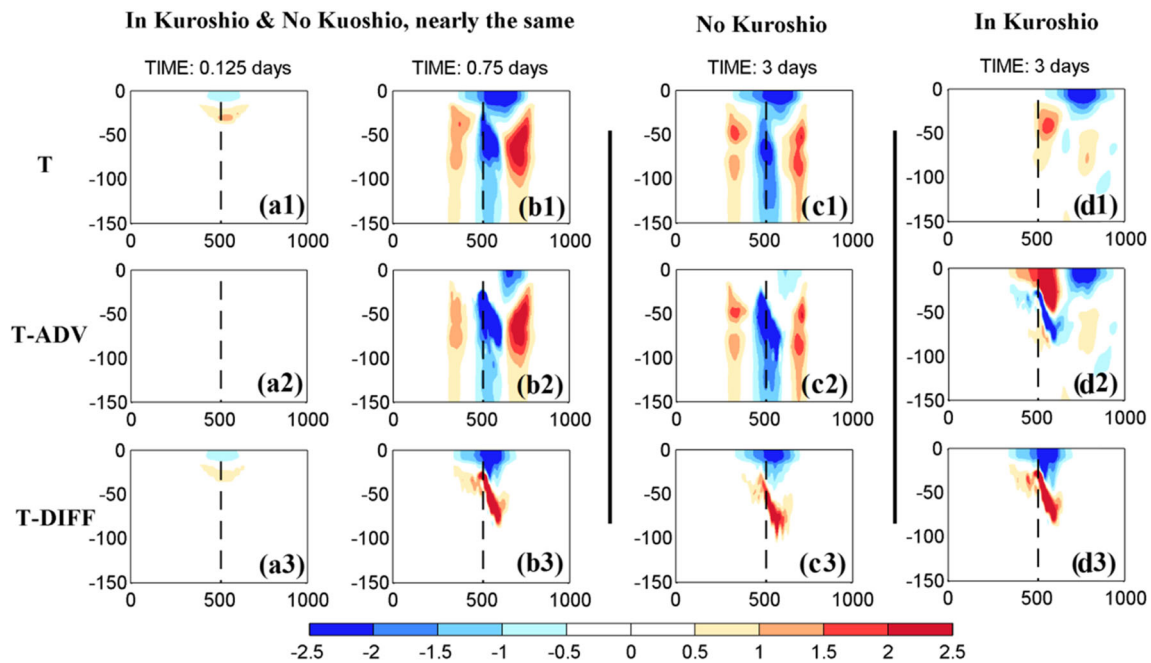
Fig. 7 Vertical sections (x-z) of temperature budget terms along the axis of the Kuroshio current during TC passage at **a1-a3** day 0.125, **b1-b3** day 0.75, **c1-c3** day 3 in the general ocean, and **d1-d3** day 3 in the Kuroshio. Initial values at day 0 are subtracted from each term for a better comparison. The budget terms of days 0.125 and 0.75 in the Kuroshio (not shown) are about the same as in the general ocean

the TC passage, the upstream downwelling-induced warm water masses are transported downstream by the Kuroshio Current, which makes the subsurface temperature cooling recover quickly.

3.4 Sensitivity experiments

The model results (control experiment) suggested that the rapid subsurface temperature warming (recovery) in the Kuroshio is essentially related to the structure of the TC wind forcing. Given that in reality, TCs usually own stronger winds on its right-hand side, we carried out a sensitivity experiment driven by an asymmetric TC. Figure 9 shows TC wind field and

corresponding results. With an asymmetric wind forcing, the warm water mass on the left-hand side of the TC center disappeared, while the one on the right-hand side remained. This implies that the occurrence of the warm water mass is directly related to the wind stress on the left-hand side.

Further, additional sensitivity experiments were carried out to test the sensitivity of the temperature changes to TC moving speed (Vs) and the Kuroshio velocity (Ug). The experiment configurations are listed in Table 3, and the results are presented in Fig. 10. It is shown that the temperature cooling is much sensitive to the TC moving speed. Compared to the control run (CT), a slow-moving TC (ST3) resulted in stronger cooling in both the general ocean and the Kuroshio mainly
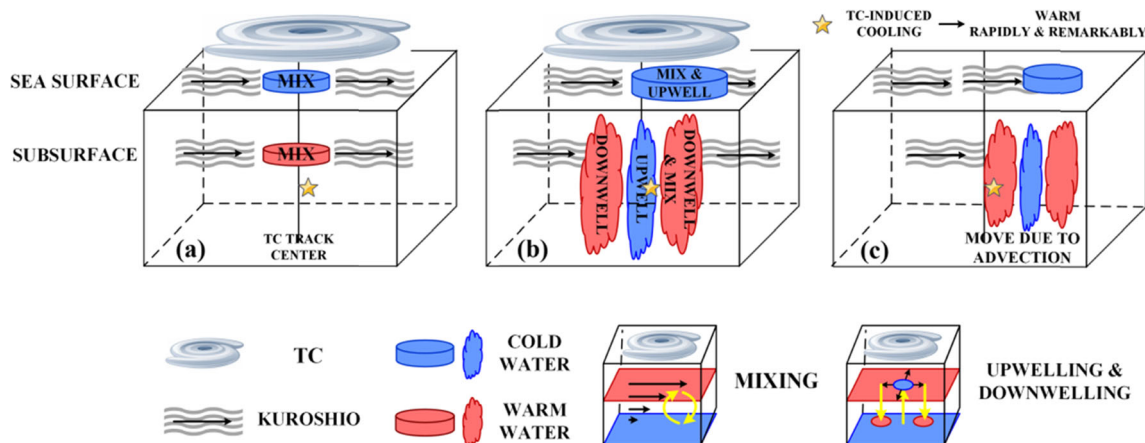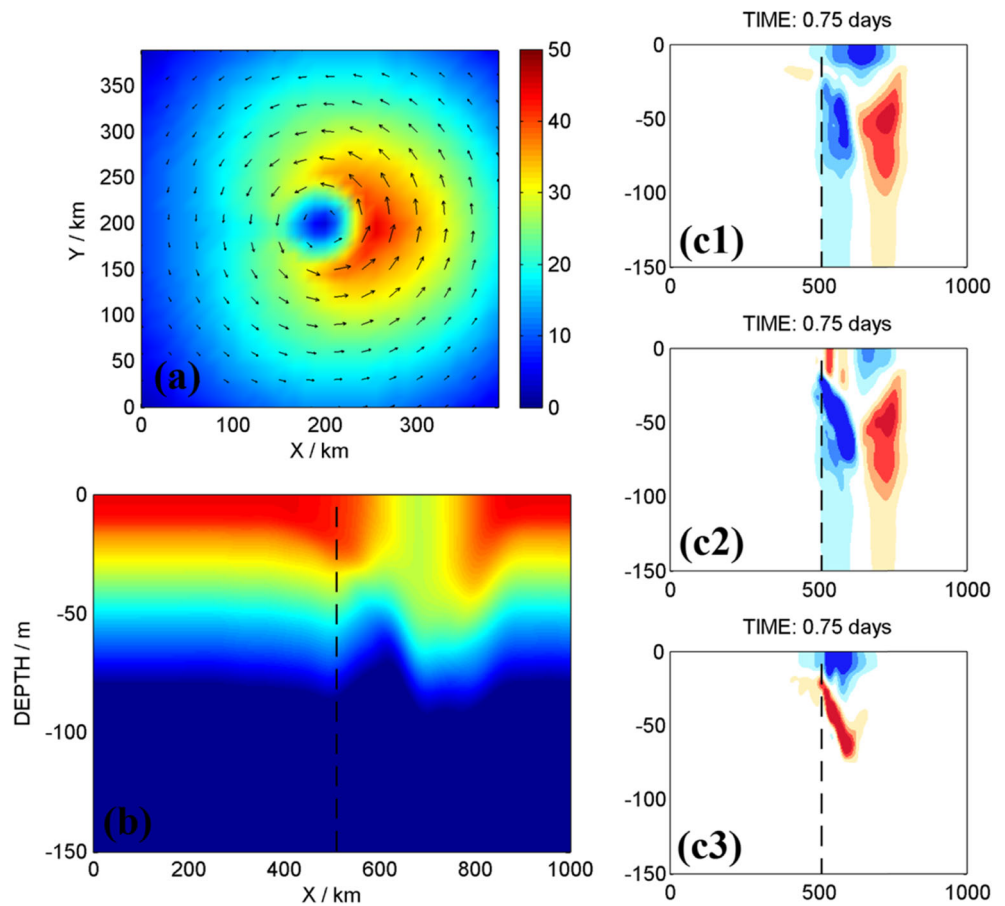

Fig. 8 Schematics of the Kuroshio response during **a** TC approaching, **b** TC arriving, and **c** TC passing over

Fig. 9 Sensitivity experiment with an asymmetric TC. **a** TC bottom wind field, **b** vertical section (x-z) of temperature changes along the axis of the Kuroshio at day 0.75, and **c1-c3** vertical sections (x-z) of temperature budget terms along the axis of the Kuroshio at day 0.75

due to sustained wind-induced vertical mixing. However, the temperature cooling recovered more rapidly in ST3, given the time period from temperature minima back to the normal (Fig. 10d1). In contrast, the temperature changes are less sensitive to the current speed of the Kuroshio. Compared to the control run (CT), the experiment with stronger Kuroshio currents (ST1) produced slightly shorter recovery time (Fig. 10b1) due to stronger advection effect.

4 Summary and discussions

Surface and subsurface temperature changes in the Kuroshio induced by tropical cyclones (TCs) were investigated using

Table 3 Sensitivity experiments for Kuroshio velocity (Ug) and TC moving speed (Vs)

CASE	Ug (m/s)	Vs (m/s)
ST1	0.825	5.5
CTR	1.1	5.5
ST2	1.375	5.5
ST3	1.1	2.75
CTR	1.1	5.5
ST4	1.1	8.25

both 10-year observational datasets (SST maps and Argo data) and temperature budget analysis of idealized numerical simulations. Although Argo data are very limited during the periods of the TC passages, they provided unique in situ measurements at the subsurface of the Kuroshio. Compared to the surface water in the Kuroshio and the general ocean, the subsurface water of the Kuroshio shows a rapid temperature warming (recovery) after a TC passage. Budget analysis on model simulations suggested that the Kuroshio subsurface water is warmed mainly by the TC-induced downwelling processes, and then transported downstream by the strong Kuroshio currents. Sensitivity experiments showed that the subsurface warm water mass is primarily produced by the TC-induced Ekman pumping (downwelling-upwelling-downwelling pattern). The recovery time of the subsurface temperature cooling is more sensitive to TC moving speeds and less sensitive to the current speed of the Kuroshio.

While most of previous studies of TC-ocean interactions were focused on the surface ocean response primarily based on satellite-derived SST maps, very few studies concerned about subsurface ocean temperature response likely due to very limited subsurface ocean measurements under severe TC conditions. Instead of focusing on the open ocean which was well understood from previous studies, this study
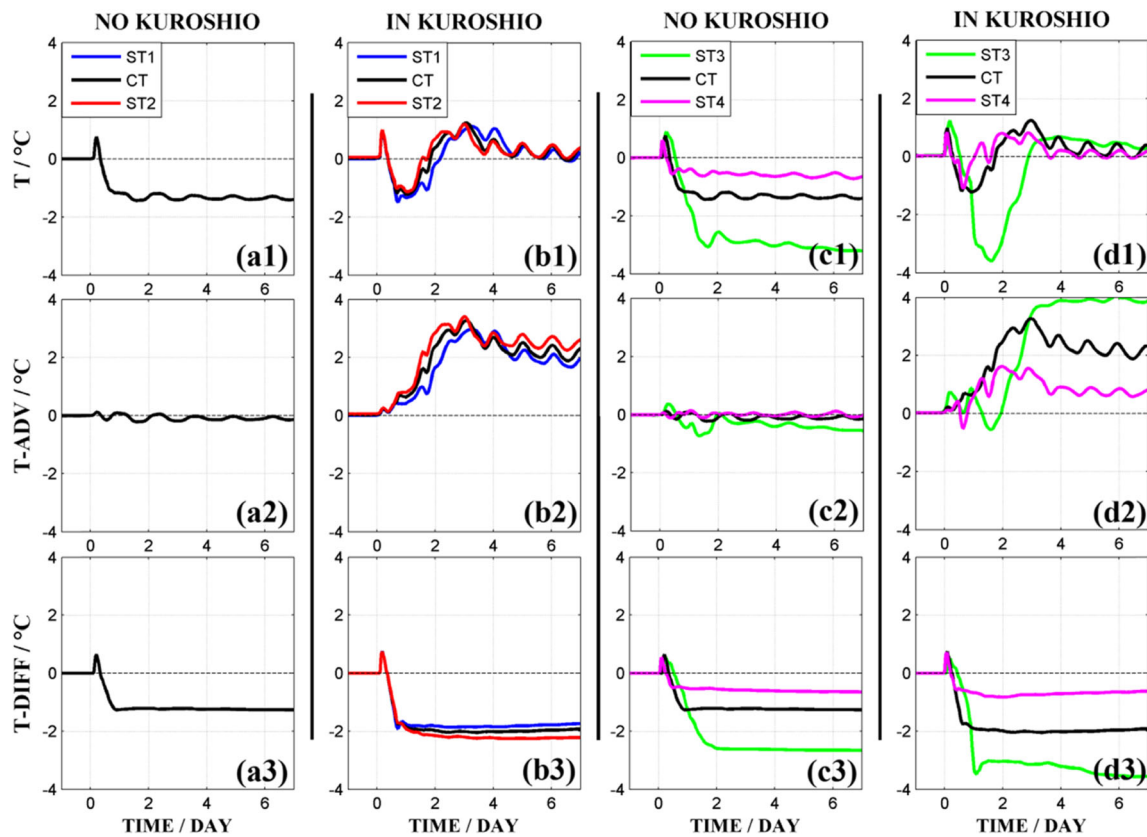
Fig. 10 Time series of temperature budget terms of the sensitivity tests (ST1-4) at 26.7-m depth **a1-a3** in the general ocean, **b1-b3** in the Kuroshio for ST1 and ST2, and **c1-c3** in the general ocean, **d1-d3** in the Kuroshio for ST3 and ST4. Control test (CT) is also marked for reference. Initial values are subtracted from each term for a better comparison

emphasized on the rapid temperature warming (recovery) at the subsurface of the Kuroshio based on the Argo temperature profiles. The observed subsurface temperature warming was well simulated and qualitatively explained by the model simulations, even though the model was configured with an idealized TC and Kuroshio current. This implies that the observed unusual subsurface temperature changes might be a fundamental process during the TC-Kuroshio interaction.

One of our previous studies extensively examined the upper ocean response of the Kuroshio to typhoon Megi (Wei et al. 2014). In that paper, we found that in the case of typhoon Megi, the ocean surface temperature cooling in the Kuroshio is determined by the vertical mixing and baroclinic pressure work of the current. The present study with the Argo data and the sensitivity tests supplemented (Wei et al. 2014) with a focus on the subsurface temperature changes and further demonstrated the entire vertical section of temperature changes in the Kuroshio during a TC passage. In summary, the temperature changes at surface Kuroshio are dominated by the wind-induced vertical mixing and the baroclinic Kuroshio currents, while the subsurface temperature changes are primarily dominated by the TC-induced Ekman pumping but quickly advected by the strong Kuroshio currents.

References

Andres M et al (2008) Study of the Kuroshio/Ryukyu Current system based on satellite-altimeter and in situ measurements. J Oceanogr 64(6):937–950

Cione JJ, Uhlhorn EW (2003) Sea surface temperature variability in hurricanes: implications with respect to intensity change. Mon Weather Rev 131(8):1783–1796

Flather RA (1976) A tidal model of the northwest European continental shelf. Mem Soc R Sci Liege 10(6):141–164

Guo X et al (2003) A triply nested ocean model for simulating the Kuroshio-Roles of horizontal resolution on JEBAR. J Phys Oceanogr 33(1):146–169

Hsueh Y (2000) The Kuroshio in the East China Sea. J Mar Syst 24(1): 131–139

Huang PS, Sanford TB, Imberger J (2009) Heat and turbulent kinetic energy budgets for surface layer cooling induced by the passage of Hurricane Frances (2004). J Geophys Res 114, C12023. doi:10. 1029/2009JC005603

Ichikawa H, Beardsley RC (2002) The current system in the Yellow and East China Seas. J Oceanogr 58(1):77–92

Jacob SD, Shay LK, Mariano AJ, Black PG (2000) The 3D oceanic mixed layer response to Hurricane Gilbert. J Phys Oceanogr 30: 1407–1429

Jaimes B, Shay LK (2009) Mixed layer cooling in mesoscale oceanic eddies during Hurricanes Katrina and Rita. Mon Weather Rev 137: 4188–4207

Jullien S, Menkes CE, Marchesiello P, Jourdain NC, Lengaigne M, Koch-Larrouy A, Lefevre J, Vincent EM, Faure V (2012) Impact of tropical cyclones on the heat budget of the south pacific ocean. J Phys Oceanogr 42(11):1882–1906. doi:10.1175/jpo-d-11-0133.1

Liu LL et al (2008) The mechanical energy input to the ocean induced by tropical cyclones. J Phys Oceanogr 38(6):1253–1266

Miyazawa Y et al (2004) Roles of mesoscale eddies in the Kuroshio paths. J Phys Oceanogr 34(10):2203–2222

Morimoto A et al (2009) Movement of the Kuroshio axis to the northeast shelf of Taiwan during typhoon events. Estuar Coast Shelf Sci 82(3): 547–552

Nagano A et al (2007) Current system east of the Ryukyu Islands. J Geophys Res: Oceans (1978–2012), 112(C6)

Oey LY et al (2006) Loop current warming by Hurricane Wilma. Geophys Res Lett 33(8)

Park JJ et al (2011) Argo array observation of ocean heat content changes induced by tropical cyclones in the north Pacific. J Geophys Res: Oceans (1978–2012), 116(C12)

Price JF (1981) Upper ocean response to a hurricane. J Phys Oceanogr 11(2):153–175

Price JF et al (1994) Forced stage response to a moving hurricane. J Phys Oceanogr 24(2):233–260

Sakaida F et al (1998) Sea surface cooling caused by typhoons in the Tohoku Area in August 1989. J Geophys Res Oceans 103(C1): 1053–1065

Sanford TB et al (2011), Upper-ocean response to hurricane frances (2004) Observed by Profiling EM-APEX Floats**. J Phys Oceanogr 41(6)

Shay LK, Black PG, Mariano AJ, Hawkins JD, Elsberry RL (1992) Upper ocean response to Hurricane Gilbert. J Geophys Res 97, 20 227–20 248

Shay LK et al (2000) Effects of a warm oceanic feature on Hurricane Opal. Mon Weather Rev 128(5)

Shchepetkin AF, McWilliams JC (2005) The regional oceanic modeling system (ROMS): a split-explicit, free-surface, topography-following-coordinate oceanic model. Ocean Model 9(4):347–404

Small RJ et al (2008) Air–sea interaction over ocean fronts and eddies. Dyn Atmos Oceans 45(3):274–319

Sriver RL, Huber M (2007) Observational evidence for an ocean heat pump induced by tropical cyclones. Nature 447(7144):577–580

Sun L et al (2012) Ocean responses to Typhoon Namtheun explored with Argo floats and multiplatform satellites. Atmos Ocean 50(sup1):15–26

Tseng Y et al (2012) Validation of the Kuroshio Current system in the dual-domain Pacific Ocean model framework. Prog Oceanogr 105: 102–124

Uhlhorn EW, Shay LK (2012) Loop current mixed layer energy response to Hurricane Lili (2002). Part I: observations. J Phys Oceanogr 42(3):400–419

Uhlhorn EW, Shay LK (2013) Loop current mixed layer energy response to Hurricane Lili (2002). Part II: idealized numerical simulations. J Phys Oceanogr

Vincent EM, Lengaigne M, Madec G, Vialard J, Samson G, Jourdain N, Menkes CE, Jullien S (2012) Processes setting the characteristics of sea surface cooling induced by tropical cyclones. J Geophys Res 117, C02020. doi:10.1029/2011JC007396

Vissa NK et al (2012) Response of Upper Ocean during passage of MALA cyclone utilizing ARGO data. Int J Appl Earth Obs Geoinf 14(1):149–159

Wei J, Liu X, Wang D (2014) Dynamic and thermal responses of the Kuroshio to typhoon Megi (2004). Geophys Res Lett 41, doi:10.1002/2014GL061706

Wu Q, Chen D (2012) Typhoon-Induced Variability of the Oceanic Surface Mixed Layer Observed by Argo Floats in the Western North Pacific Ocean. Atmos Ocean 50(sup1):4–14

Wu CR et al (2008) Air-sea interaction between tropical cyclone Nari and Kuroshio. Geophys Res Lett 35(12)

Zheng ZW et al (2008) Importance of pre-existing oceanic conditions to upper ocean response induced by Super Typhoon Hai-Tang. Geophys Res Lett 35(20)